

## Triplet of Nuclear Scissors Modes

**I.V. Molodtsova<sup>1</sup>, E.B. Balbutsev<sup>1</sup>, P. Schuck<sup>2</sup>, A.V. Sushkov<sup>1</sup>,  
N.Yu. Shirikova<sup>1</sup>**

<sup>1</sup>Bogoliubov Laboratory of Theoretical Physics,  
Joint Institute for Nuclear Research, Dubna, 141980, Russia

<sup>2</sup>Institut de Physique Nucléaire, IN2P3-CNRS, Université Paris-Sud,  
F-91406 Orsay Cédex, France; Univ. Grenoble Alpes, CNRS, LPMMC,  
38000 Grenoble, France

**Abstract.** The low energy  $M1$  excitations are studied within the Time Dependent Hartree-Fock-Bogoliubov (TDHFB) approach. The solution of TDHFB equations by the Wigner Function Moments method predicts three types of scissors modes. Together with the conventional scissors mode generated by the counter-rotation of protons against neutrons, two new modes arise due to spin degrees of freedom (“spin” scissors). Two states fall into the energy range of  $2.7 < E < 3.7$  MeV, adopted for the scissors mode. The lowest one generates a remarkable  $M1$  strength below the conventional energy range. The results of calculations for mean excitation energies and summed excitation strengths of the scissors resonance in rare earth nuclei are presented. The main focus is on the low-lying magnetic dipole strength distribution in <sup>160,162,164</sup>Dy isotopes. A comparison with the results of systematic calculations within the Quasiparticle-Phonon Nuclear Model (QPNM) and with the data for integrated scissors resonance strength reported from nuclear resonance fluorescence and data of photon-neutron measurement from the Oslo-type experiments is discussed.

### 1 Introduction

The magnetic dipole ( $M1$ ) response of atomic nuclei, as one of their fundamental features, is the subject of in-depth experimental and theoretical study since it provides valuable information on the structure of the nucleus and the nature of nuclear forces. The nuclear scissors mode was predicted as a counter-rotation of protons against neutrons in deformed nuclei [1–3] and detected as a low-lying magnetic dipole excitation, typically distributed over several  $1^+$  states in the energy range between 2 and 4 MeV. Extensive systematic of the scissors mode has been accumulated in the nuclear resonance fluorescence (NRF) experiments (for a review, see [4] and references there). It was found that the integrated  $M1$  strength depends quadratically on the deformation parameter  $\delta$  with a typical value  $\sum B(M1) \simeq 3 \mu_N^2$  in the most rare-earth nuclei. In recent years, a wealth of information about the  $M1$  strength distribution has been provided from an analysis based on the  $\gamma$ -ray strength function in the quasicontinuum region of

excited nuclei extracted from  $(\gamma, n)$  [5] and  $(n, \gamma)$  [6] reactions. In these experiments, systematic low-energy enhancement of dipole magnetic strength was observed.

In the paper [7] the WFM method was applied for the first time to solve the Time Dependent Hartree-Fock equations including spin dynamics. The scissors mode is a rotational mode of isovector character. For this reason, the equations have been solved in terms of the isoscalar and isovector variables, with neglect of the coupling terms. The most remarkable result was the prediction of a new type of nuclear collective motion: rotational oscillations of "spin-up" nucleons with respect of "spin-down" nucleons (the "spin" scissors mode). This new type of nuclear scissors complements the familiar (orbital) scissors mode. Subsequent accounting of pair correlations allowed to improve considerably the quantitative agreement between the results of WFM theory and experiment [8,9].

Solving the equations for the proton and neutron systems together, without isovector-isoscalar decoupling, leads to appearance of another spin scissors branch. The existence of three states of scissors can be intuitively understood from combinatorial considerations – there are only three ways to divide the four different kinds of objects (spin up and spin down protons and neutrons in our case) into two pairs.

## 2 Model and WFM Method

The basis of the WFM method is the Time-Dependent Hartree-Fock-Bogoliubov (TDHFB) equation in matrix formulation [10]:

$$i\hbar\dot{\mathcal{R}} = [\mathcal{H}, \mathcal{R}] \quad (1)$$

with

$$\mathcal{R} = \begin{pmatrix} \hat{\rho} & -\hat{\kappa} \\ -\hat{\kappa}^\dagger & 1 - \hat{\rho}^* \end{pmatrix}, \quad \mathcal{H} = \begin{pmatrix} \hat{h} & \hat{\Delta} \\ \hat{\Delta}^\dagger & -\hat{h}^* \end{pmatrix} \quad (2)$$

The normal density matrix  $\hat{\rho}$  and Hamiltonian  $\hat{h}$  are hermitian whereas the abnormal density  $\hat{\kappa}$  and the pairing gap  $\hat{\Delta}$  are skew symmetric:  $\hat{\kappa}^\dagger = -\hat{\kappa}^*$ ,  $\hat{\Delta}^\dagger = -\hat{\Delta}^*$ . While we do not specify the isospin indices in order to make formulae more transparent. Let us consider matrix form of (1) in coordinate space keeping spin indices  $\{s, s'\} = \{\uparrow, \downarrow\}$  (here  $\uparrow$  denotes  $s = 1/2$ ,  $\downarrow$  denotes  $s = -1/2$ ) with compact notation  $X_{rr'}^{ss'} \equiv \langle \mathbf{r}, s | \hat{X} | \mathbf{r}', s' \rangle$ . Then the set of

### Triplet of Nuclear Scissors Modes

TDHFB equations with specified spin indices reads [9]:

$$\begin{aligned}
i\hbar\dot{\rho}_{rr''}^{\uparrow\uparrow} &= \int d^3r' (h_{rr'}^{\uparrow\uparrow}\rho_{r'r''}^{\uparrow\uparrow} - \rho_{rr'}^{\uparrow\uparrow}h_{r'r''}^{\uparrow\uparrow} + h_{rr'}^{\uparrow\downarrow}\rho_{r'r''}^{\downarrow\uparrow} - \rho_{rr'}^{\uparrow\downarrow}h_{r'r''}^{\downarrow\uparrow} \\
&\quad - \Delta_{rr'}^{\uparrow\downarrow}\kappa_{r'r''}^{\uparrow\downarrow} + \kappa_{rr'}^{\uparrow\downarrow}\Delta_{r'r''}^{\uparrow\downarrow}), \\
i\hbar\dot{\rho}_{rr''}^{\uparrow\downarrow} &= \int d^3r' (h_{rr'}^{\uparrow\uparrow}\rho_{r'r''}^{\uparrow\downarrow} - \rho_{rr'}^{\uparrow\uparrow}h_{r'r''}^{\uparrow\downarrow} + h_{rr'}^{\uparrow\downarrow}\rho_{r'r''}^{\downarrow\downarrow} - \rho_{rr'}^{\uparrow\downarrow}h_{r'r''}^{\downarrow\downarrow}), \\
i\hbar\dot{\rho}_{rr''}^{\downarrow\uparrow} &= \int d^3r' (h_{rr'}^{\downarrow\uparrow}\rho_{r'r''}^{\uparrow\uparrow} - \rho_{rr'}^{\downarrow\uparrow}h_{r'r''}^{\uparrow\uparrow} + h_{rr'}^{\downarrow\downarrow}\rho_{r'r''}^{\downarrow\uparrow} - \rho_{rr'}^{\downarrow\downarrow}h_{r'r''}^{\downarrow\uparrow}), \\
i\hbar\dot{\rho}_{rr''}^{\downarrow\downarrow} &= \int d^3r' (h_{rr'}^{\downarrow\uparrow}\rho_{r'r''}^{\uparrow\downarrow} - \rho_{rr'}^{\downarrow\uparrow}h_{r'r''}^{\uparrow\downarrow} + h_{rr'}^{\downarrow\downarrow}\rho_{r'r''}^{\downarrow\downarrow} - \rho_{rr'}^{\downarrow\downarrow}h_{r'r''}^{\downarrow\downarrow}) \\
&\quad - \Delta_{rr'}^{\downarrow\uparrow}\kappa_{r'r''}^{\downarrow\uparrow} + \kappa_{rr'}^{\downarrow\uparrow}\Delta_{r'r''}^{\downarrow\uparrow}), \\
i\hbar\dot{\kappa}_{rr''}^{\uparrow\downarrow} &= \int d^3r' (h_{rr'}^{\uparrow\uparrow}\kappa_{r'r''}^{\uparrow\downarrow} + \kappa_{rr'}^{\uparrow\downarrow}h_{r'r''}^{*\downarrow\downarrow} + \Delta_{rr'}^{\uparrow\downarrow}\rho_{r'r''}^{*\downarrow\downarrow} + \rho_{rr'}^{\uparrow\uparrow}\Delta_{r'r''}^{\uparrow\downarrow}) \\
&\quad - \Delta_{rr''}^{\uparrow\downarrow}, \\
i\hbar\dot{\kappa}_{rr''}^{\downarrow\uparrow} &= \int d^3r' (h_{rr'}^{\downarrow\downarrow}\kappa_{r'r''}^{\downarrow\uparrow} + \kappa_{rr'}^{\downarrow\uparrow}h_{r'r''}^{*\uparrow\uparrow} + \Delta_{rr'}^{\downarrow\uparrow}\rho_{r'r''}^{*\uparrow\uparrow} + \rho_{rr'}^{\downarrow\downarrow}\Delta_{r'r''}^{\downarrow\uparrow}) \\
&\quad - \Delta_{rr''}^{\downarrow\uparrow}.
\end{aligned} \tag{3}$$

This set of equations must be complemented by the complex conjugated equations. We work with the Wigner transform [10] of equations (3). The relevant mathematical details can be found in [8, 9]. The functions  $f^{ss'}(\mathbf{r}, \mathbf{p}, t)$ ,  $\kappa^{ss'}(\mathbf{r}, \mathbf{p}, t)$ ,  $\Delta^{ss'}(\mathbf{r}, \mathbf{p}, t)$  and  $h^{ss'}(\mathbf{r}, \mathbf{p}, t)$  are the Wigner transforms of  $\rho_{rr'}^{ss'}$ ,  $\kappa_{rr'}^{ss'}$ ,  $\Delta_{rr'}^{ss'}$  and  $h_{rr'}^{ss'}$ , respectively. As a result, we obtain a set of 12 equations, which is solved by the method of moments in a small amplitude approximation. To this end all functions  $f^{ss'}(\mathbf{r}, \mathbf{p}, t)$  and  $\kappa^{ss'}(\mathbf{r}, \mathbf{p}, t)$  are divided into equilibrium part and deviation (variation):  $f^{ss'}(\mathbf{r}, \mathbf{p}, t) = f_{\text{eq}}^{ss'}(\mathbf{r}, \mathbf{p}) + \delta f^{ss'}(\mathbf{r}, \mathbf{p}, t)$ ,  $\kappa^{ss'}(\mathbf{r}, \mathbf{p}, t) = \kappa_{\text{eq}}^{ss'}(\mathbf{r}, \mathbf{p}) + \delta \kappa^{ss'}(\mathbf{r}, \mathbf{p}, t)$ . Then equations are linearized neglecting quadratic in  $\delta f$  and  $\delta \kappa$  terms [8]. Following the papers [7] in the next step we write obtained equations in terms of spin-scalar  $f^+ = f^{\uparrow\uparrow} + f^{\downarrow\downarrow}$  and spin-vector  $f^- = f^{\uparrow\uparrow} - f^{\downarrow\downarrow}$  functions.

The microscopic Hamiltonian of the model, harmonic oscillator with spin orbit potential plus separable quadrupole-quadrupole and spin-spin residual interactions, is given by

$$H = \sum_{i=1}^A \left[ \frac{\hat{\mathbf{p}}_i^2}{2m} + \frac{1}{2}m\omega^2\mathbf{r}_i^2 - \eta\hat{\mathbf{l}}_i\hat{\mathbf{S}}_i \right] + H_{qq} + H_{ss}, \tag{4}$$

with

$$H_{qq} = \sum_{\mu=-2}^2 (-1)^\mu \left\{ \bar{\kappa} \sum_i^Z \sum_j^N + \frac{\kappa}{2} \left[ \sum_{\substack{i,j \\ (i \neq j)}}^Z + \sum_{\substack{i,j \\ (i \neq j)}}^N \right] \right\} q_{2-\mu}(\mathbf{r}_i) q_{2\mu}(\mathbf{r}_j),$$

$$H_{ss} = \sum_{\mu=-1}^1 (-1)^\mu \left\{ \bar{\chi} \sum_i^Z \sum_j^N + \frac{\chi}{2} \left[ \sum_{\substack{i,j \\ (i \neq j)}}^Z + \sum_{\substack{i,j \\ (i \neq j)}}^N \right] \right\} \hat{S}_{-\mu}(i) \hat{S}_\mu(j) \delta(\mathbf{r}_i - \mathbf{r}_j),$$

where  $q_{2\mu}(\mathbf{r})$  is a quadrupole operator,  $\hat{S}_\mu$  are spin matrices [11],  $\kappa$ ,  $\bar{\kappa}$  and  $\chi$ ,  $\bar{\chi}$  are strength constants,  $N$  and  $Z$  – numbers of neutrons and protons, respectively.

Integrating the set of equations for the  $\delta f_\tau^\zeta(\mathbf{r}, \mathbf{p}, t)$  and  $\delta \kappa_\tau^\zeta(\mathbf{r}, \mathbf{p}, t)$  over phase space with the weights  $\{r \otimes p\}_{\lambda\mu}$ ,  $\{r \otimes r\}_{\lambda\mu}$ ,  $\{p \otimes p\}_{\lambda\mu}$  and 1 one gets dynamic equations for the following second-order moments that are collective variables:

$$\begin{aligned} \mathcal{L}_{\lambda\mu}^{\tau\zeta}(t) &= (2\pi\hbar)^{-3} \int d\mathbf{r} \int d\mathbf{p} \{r \otimes p\}_{\lambda\mu} \delta f_\tau^\zeta(\mathbf{r}, \mathbf{p}, t), \\ \mathcal{R}_{\lambda\mu}^{\tau\zeta}(t) &= (2\pi\hbar)^{-3} \int d\mathbf{r} \int d\mathbf{p} \{r \otimes r\}_{\lambda\mu} \delta f_\tau^\zeta(\mathbf{r}, \mathbf{p}, t), \\ \mathcal{P}_{\lambda\mu}^{\tau\zeta}(t) &= (2\pi\hbar)^{-3} \int d\mathbf{r} \int d\mathbf{p} \{p \otimes p\}_{\lambda\mu} \delta f_\tau^\zeta(\mathbf{r}, \mathbf{p}, t), \\ \mathcal{F}^{\tau\zeta}(t) &= (2\pi\hbar)^{-3} \int d\mathbf{r} \int d\mathbf{p} \delta f_\tau^\zeta(\mathbf{r}, \mathbf{p}, t), \\ \tilde{\mathcal{L}}_{\lambda\mu}^{\tau\zeta}(t) &= (2\pi\hbar)^{-3} \int d\mathbf{r} \int d\mathbf{p} \{r \otimes p\}_{\lambda\mu} \delta \kappa_\tau^{\uparrow\downarrow}(\mathbf{r}, \mathbf{p}, t), \\ \tilde{\mathcal{R}}_{\lambda\mu}^{\tau\zeta}(t) &= (2\pi\hbar)^{-3} \int d\mathbf{r} \int d\mathbf{p} \{r \otimes r\}_{\lambda\mu} \delta \kappa_\tau^{\uparrow\downarrow}(\mathbf{r}, \mathbf{p}, t), \\ \tilde{\mathcal{P}}_{\lambda\mu}^{\tau\zeta}(t) &= (2\pi\hbar)^{-3} \int d\mathbf{r} \int d\mathbf{p} \{p \otimes p\}_{\lambda\mu} \delta \kappa_\tau^{\uparrow\downarrow}(\mathbf{r}, \mathbf{p}, t), \end{aligned} \quad (5)$$

where  $\zeta = +, -, \uparrow\downarrow, \downarrow\uparrow$  is the spin index,  $\tau$  is the isospin index,  $\{r \otimes p\}_{\lambda\mu} = \sum_{\sigma,\nu} C_{1\sigma,1\nu}^{\lambda\mu} r_\sigma p_\nu$  [11]. It is convenient to rewrite the coupled dynamical nonlinear equations for protons ( $\tau = p$ ) and neutrons ( $\tau = n$ ) in terms of isoscalar  $\mathcal{X}_{\lambda\mu}^\zeta = \mathcal{X}_{\lambda\mu}^{n\zeta} + \mathcal{X}_{\lambda\mu}^{p\zeta}$  and isovector  $\bar{\mathcal{X}}_{\lambda\mu}^\zeta = \mathcal{X}_{\lambda\mu}^{n\zeta} - \mathcal{X}_{\lambda\mu}^{p\zeta}$  variables, where  $\mathcal{X} = \{\mathcal{R}, \mathcal{L}, \mathcal{P}\}$ .

The physical meaning of most collective variables is obvious:  $\mathcal{R}_{2\mu}^+$  is a variation of quadrupole moment of the nucleus and  $\mathcal{R}_{00}^+$  is a variation of mean square radius,  $\mathcal{P}_{2\mu}^+$  and  $\mathcal{P}_{00}^+$  are variations of quadrupole moment and mean square radius in a momentum space. The variables  $\mathcal{L}_{\lambda\mu}^\zeta$  describe the coupling of momentum and coordinate space,  $\mathcal{L}_{1\mu}^+$  is a variation of orbital angular momentum.

### Triplet of Nuclear Scissors Modes

To describe the scissors mode with quantum number  $K^\pi = 1^+$ , only a part of the dynamic equations with  $\mu = 1$  is required. Imposing the time evolution via  $e^{i\Omega t}$  for all variables allows to transform the system of dynamical equations into a set of algebraic equations. Eigenfrequencies  $\Omega$  are found as solutions of its secular equation. As a result, we obtain a system of 44 coupled isovector and isoscalar equations of the first order in time, which can be reduced to 22 equations of the second order in time. Excluding the integrals of motion we obtain 14 eigenvalue solutions.

### 3 Results of Calculations and Discussion

The results of calculations are presented in the Table 1, where the energies, magnetic dipole and electric quadrupole strength are shown for  $^{164}\text{Dy}$ . The corresponding values obtained from solving the coupled isovector and isoscalar equations are shown in the columns marked I. As can be seen from the Table,

Table 1. The results of WFM calculations for  $^{164}\text{Dy}$ : energies  $E_i$ , magnetic dipole  $B(M1)_i$  and electric quadrupole  $B(E2)_i$  strength. I – solutions of the system of coupled equations, II – solutions of decoupled isovector and isoscalar equations: IS – isoscalar, IV – isovector.

$i$	$E_i, \text{MeV}$		$B(M1)_i, \mu_N^2$		$B(E2)_i, \text{W.u.}$	
	I	II	I	II	I	II
1	1.47	1.29 <sup>(IS)</sup>	0.17	0.01 <sup>(IS)</sup>	25.44	53.25 <sup>(IS)</sup>
2	2.20	2.44 <sup>(IV)</sup>	1.76	2.03 <sup>(IV)</sup>	3.30	0.34 <sup>(IV)</sup>
3	2.87	2.62 <sup>(IS)</sup>	2.24	0.09 <sup>(IS)</sup>	0.34	2.91 <sup>(IS)</sup>
4	3.59	3.35 <sup>(IV)</sup>	1.56	1.36 <sup>(IV)</sup>	4.37	1.62 <sup>(IV)</sup>
5	10.92	10.94 <sup>(IS)</sup>	0.04	0.00 <sup>(IS)</sup>	50.37	55.12 <sup>(IS)</sup>
6	13.10	14.04 <sup>(IV)</sup>	0.00	0.00 <sup>(IV)</sup>	2.85	2.78 <sup>(IV)</sup>
7	15.42	14.60 <sup>(IS)</sup>	0.07	0.06 <sup>(IS)</sup>	0.57	0.48 <sup>(IS)</sup>
8	15.55	15.88 <sup>(IV)</sup>	0.00	0.00 <sup>(IV)</sup>	1.12	0.55 <sup>(IV)</sup>
9	16.78	16.46 <sup>(IS)</sup>	0.06	0.07 <sup>(IS)</sup>	0.53	0.36 <sup>(IS)</sup>
10	17.69	17.69 <sup>(IV)</sup>	0.01	0.00 <sup>(IV)</sup>	0.68	0.45 <sup>(IV)</sup>
11	17.91	17.90 <sup>(IS)</sup>	0.00	0.00 <sup>(IS)</sup>	0.53	0.51 <sup>(IS)</sup>
12	18.22	18.22 <sup>(IV)</sup>	0.13	0.18 <sup>(IV)</sup>	0.89	1.85 <sup>(IV)</sup>
13	19.32	19.32 <sup>(IS)</sup>	0.08	0.10 <sup>(IS)</sup>	0.61	0.97 <sup>(IS)</sup>
14	21.26	21.29 <sup>(IV)</sup>	2.03	2.47 <sup>(IV)</sup>	21.60	31.38 <sup>(IV)</sup>

the three low-lying states (with  $i = 2, 3, 4$ ) manifest magnetic nature. Among the high-lying states,  $\mu = 1$  branches of isoscalar ( $i = 5$ ) and isovector ( $i = 14$ ) Giant Quadrupole Resonances are distinguished by a large  $B(E2)$  values. The lowest electric level has a complicated origin and this is a topic for future research. Here the focus is on the states of scissors nature.

For further analysis, we neglect the terms coupling the isovector and isoscalar systems. In this case, the equations splits into two independent subsystems. The solutions of decoupled isovector (IV) and isoscalar (IS) equations are presented in the columns II of the Table 1. The effect of the coupling terms was evaluated in [12]. Comparing I and II columns, we see that the high-lying levels are less sensitive to decoupling. The most remarkable change happens with third low-lying state – it is visibly loses the magnetic force.

The decoupled equations give additional useful information. In this case it is possible to track the variables that are predominantly responsible for the generation of the individual eigenvalues. These variables are shown in the first column of the Table 2 for the three low-lying states under discussion. All these states

Table 2. Calculated energies  $E_i$  and magnetic dipol  $B(M1)_i$  strength for  $^{164}\text{Dy}$ .

	Decoupled equations		Coupled equations	
	$E_i, \text{MeV}$	$B(M1)_i, \mu_N^2$	$E_i, \text{MeV}$	$B(M1)_i, \mu_N^2$
$\bar{\mathcal{L}}_{11}^-$	2.44	2.03	2.20	1.76
$\mathcal{L}_{11}^-$	2.62	0.09	2.87	2.24
$\bar{\mathcal{L}}_{11}^+$	3.35	1.36	3.59	1.56

are generated by oscillations of the orbital angular momenta. The variable  $\bar{\mathcal{L}}_{11}^+$  generates isovector (spin-scalar) scissors – this is conventional orbital scissors mode.  $\mathcal{L}_{11}^-$ ,  $\bar{\mathcal{L}}_{11}^-$  generate **spin-vector** scissors (isoscalar and isovector, respectively). These two states are the **spin scissors mode**. It must be emphasized that

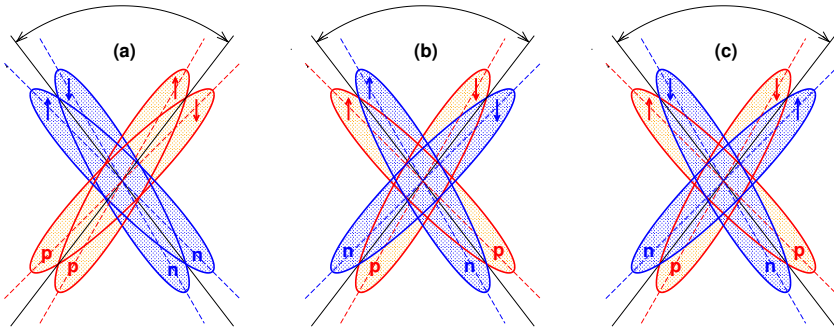


Figure 1. Schematic representation of three scissors modes: (a) spin-scalar isovector (conventional, orbital scissors), (b) spin-vector isoscalar (spin scissors), (c) spin-vector isovector (spin scissors). Arrows show the direction of spin projections; p – protons, n – neutrons. The small angle spread between the various distributions is only for presentation purposes. In reality the distributions are perfectly overlapping. The isovector and isoscalar marks should be understood approximately, because both these types of motion are coupled.

### Triplet of Nuclear Scissors Modes

all three scissors modes have an underlying **orbital nature**, because all are generated by the same type of collective variables – the orbital angular momenta. Figure 1 shows a schematic representation of these modes: (a) spin-up and spin-down protons oscillate versus the corresponding neutrons – spin-scalar isovector (conventional scissors), (b) protons and neutrons, both spin-up oscillate versus same with spin-down – spin-vector isoscalar (spin scissors), (c) protons spin-up with neutrons spin-down oscillate versus protons spin-down with neutrons spin-up – spin-vector isovector (spin scissors). Both spin scissors exist only due to spin degrees of freedom. If we remove the arrows from the picture, nothing will change for the conventional scissors (a). However figures (b) and (c) in this case become identical and senseless, because the division of neutrons and protons in two parts becomes pointless. Calculations without an artificial decoupling produce three scissors states of mixed nature (right panel of the Table 2). Coupling particularly strongly overlaps two spin-vector levels at the energies of 2.20 MeV and 2.87 MeV. Analysis of the flow distributions [7] confirms the rotational nature of all three states.

Comparing the theoretical results with the available experimental data, we encounter summing interval conventions, adopted for the scissors mode. It is assumed that scissors mode includes only the states in a certain energy range:  $2.7 < E < 3.7$  MeV for  $Z < 68$  and  $2.4 < E < 3.7$  MeV for  $Z \geq 68$  [13] or  $2.5 < E < 4.0$  MeV for  $82 \leq N \leq 126$  [14]. The scissors resonance in  $^{164}\text{Dy}$  is especially interesting. There are two groups of strong  $M1$  excitations around 2.6 and 3.1 MeV, respectively, were detected by the NRF experiment [15] here. Only the upper group falls within the conditional interval and refers to the scissors mode. This situation has already been analyzed in detail in [12]. The results of WFM calculations allow one to clarify the origin of both groups. Table 3 demonstrates that the energy centroid  $\bar{E}$  and summed  $\sum B(M1)$ -value of the lower group of the experimental  $1^+$  states agree very well with the calculated  $E$  and  $B(M1)$  of the first spin-vector level. The respective values of the higher group are in agreement with the energy centroid and summed  $B(M1)$  of two remaining (higher in energy) scissors. Summation over all transition energies also gives an excellent agreement with the theory (last row of the Table).

Table 3. The energies  $E$  and excitation probabilities  $B(M1)$  of three scissors are compared with experimental values  $\bar{E}$  and  $\sum B(M1)$  of two groups of  $1^+$  levels in  $^{164}\text{Dy}$  [15].

Theory (WFM)				Experiment (NRF)	
$E$ , MeV	$B(M1), \mu_N^2$	$\bar{E}$ , MeV	$\sum B(M1), \mu_N^2$	$\bar{E}$ , MeV	$\sum B(M1), \mu_N^2$
2.20	1.76	2.20	1.76	2.60	1.67(14)
2.87	2.24	3.17	3.80	3.17	3.85(31)
3.59	1.56				
		2.86	5.56	3.00	5.52(48)

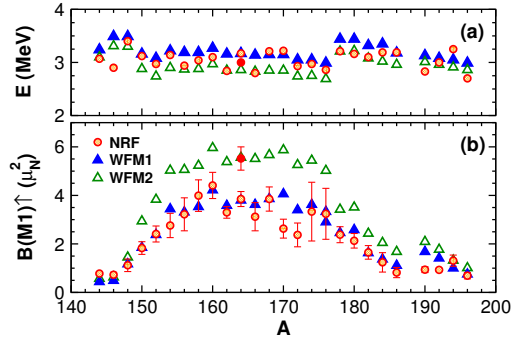


Figure 2. Calculated (WFM) and experimental (NRF) mean excitation energies (a) and summed  $M1$  strengths (b) of the scissors mode. WFM1 – the sum of two highest scissors, WFM2 – the sum of three scissors. The solid circle marks the experimental result for  $^{164}\text{Dy}$  when summed in the energy range from 2 to 4 MeV [15].

So, according to our calculations, the low-energy group of states in  $^{164}\text{Dy}$  is also a branch of the scissors mode and gives rise for the  $B(M1)$  to the full (red) dot at around  $5 \mu_N^2$  in Figure 2.

In the rest nuclei of  $N = 82 - 126$  mass region an equally significant low energy  $M1$  strength was not detected in the NRF experiments. However, WFM calculations predict the existence of comparable magnetic strength in all well-deformed nuclei of this mass region (see WFM2 in Figure 2). This prediction is supported by the systematic calculations, performed in the frame of extended RPA formalism – Quasiparticle-Phonon Nuclear Model (QPNM) [16], which also predict the remarkable  $M1$  strength below the conventional energy interval. Mean excitation energies and summed  $B(M1)$  calculated for the energy range from 2 to 4 MeV are presented in Figure 3 in comparison with WFM theory.

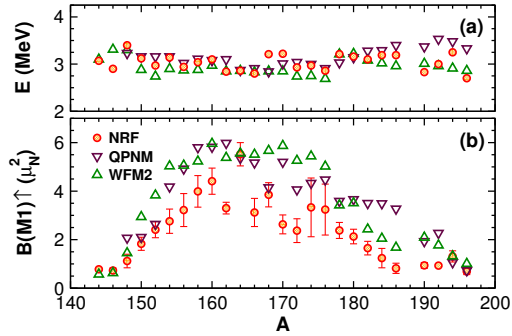


Figure 3. Calculated (within WFM and QPNM) and experimental (NRF) mean excitation energies (a) and summed  $M1$  strengths (b) of the scissors mode. QPNM – calculations in the energy range from 2 to 4 MeV, WFM2 – the sum of three scissors.

### Triplet of Nuclear Scissors Modes

Theoretical prediction is supported by the recent experimental results of photo-neutron measurements performed by the Oslo group. The authors revised their previous data on the Scissors Resonance in  $^{160-164}\text{Dy}$  isotopes obtained by the Oslo method. It was found that integration over all transition energies gives a total, summed strength value of about  $5 \mu^2$ . However, if the NRF energy limits are applied, excellent agreement with the NRF results is obtained. It is interesting to note that up to 60 percent of measured strength lies in the energy region below 2.7 MeV. All this is in excellent agreement with our calculations. The energy centroids and corresponding summed  $B(M1)$  given by the WFM theory and by the QPNM calculations are compared with experimental results from the NRF, from photo-neutron measurements (Oslo) [5] and the results obtained by the radiative capture of resonance neutrons [6] in Figure 4. The results are shown for various energy intervals. As it is seen, the theoretical results and experimental data of Oslo group are in very good overall agreement for all three Dy isotopes. It is remarkable to which extent theory and experiment agree taking the NRF as well as the Oslo averaging intervals. This yields strong support to our interpretation that there are in fact not one but three intermingled scissors modes at play: the standard one and two spin scissors which may be predominately isovector spin-vector and isoscalar spin-vector in nature.

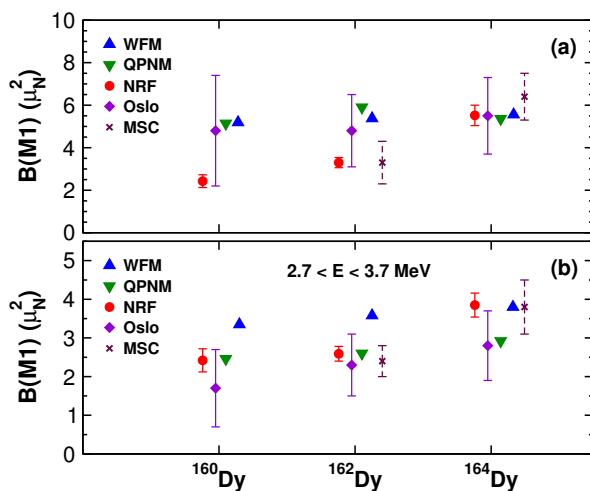


Figure 4. Comparison of the summed  $B(M1)$ -values for scissors resonance in  $^{160,162,164}\text{Dy}$  from the WFM and QPNM calculations with the experimental values from the NRF [15], photo-neutron measurements (Oslo) [5] and from multistep-cascade (MSC) measurements of  $\gamma$  decay following neutron capture [6]. Panel (a) – averaging energy intervals are 2 – 4 MeV for WFM, QPNM and NRF; 0 – 10 MeV for Oslo and MSC; (b) – averaging interval is 2.7 – 3.7 MeV, QPNM [16].

## 4 Conclusion

The dynamical equations describing the nuclear collective motion are solved without the artificial division into isovector and isoscalar parts. As a result a new type (third one) of nuclear scissors is found. Three scissor modes are the realization of three physically possible states formed by a pairwise combination of four different kinds of objects (in our case, spin up and spin down protons and neutrons). Three types of scissors can be approximately classified as isovector spin-scalar (conventional), isovector spin-vector and isoscalar spin-vector. Both spin scissors exist only due to spin degrees of freedom. The low-energy group of  $1^+$  states in  $^{164}\text{Dy}$  finds explanation within WFM method as a branch of the scissors mode (spin-vector isovector scissors). The calculated energy centroids and summarized transition probabilities of even-even Dy isotopes are in a very good agreement with the experimental results of Oslo group. The NRF data for  $^{164}\text{Dy}$  are in excellent agreement with our calculations, whereas the data for  $^{160,162}\text{Dy}$  are in a good agreement only with calculated centroids of two higher-lying states falling into the conventional energy region of scissors mode. It is likely that the 2 – 2.5 MeV energy region, where the concentration of  $M1$  strength associated with the spin scissors is expected, remains insufficiently studied. So we join the conclusion of the authors of [5]: “It is highly desirable to remeasure the Dy isotopes by performing NRF experiments using quasi-monochromatic beams in the interesting energy region between 2 and 4 MeV as done for  $^{232}\text{Th}$ .”

## References

- [1] R.R. Hilton, “A Possible Vibrational Mode in Heavy Nuclei”, *Talk presented at the Int. Conf. on Nuclear Structure*, JINR, Dubna, Russia, 1976 (unpublished).
- [2] N. Lo Iudice and F. Palumbo, *Phys. Rev. Lett.* **41** (1978) 1532.
- [3] T. Suzuki and D.J. Rowe, *Nucl. Phys. A* **289** (1977) 461.
- [4] K. Heyde, P. von Neumann-Cosel, and A. Richter, *Rev. Mod. Phys.* **82** (2010) 2365.
- [5] T. Renstrøm, *et al.*, *Phys. Rev. C* **98** (2018) 054310.
- [6] S. Valenta, *et al.*, *Phys. Rev. C* **96** (2017) 054315.
- [7] E.B. Balbutsev, I.V. Molodtsova, and P. Schuck, *Nucl. Phys. A* **872** (2011) 42.
- [8] E.B. Balbutsev, I.V. Molodtsova, and P. Schuck, *Phys. Rev. C* **91** (2015) 064312.
- [9] E.B. Balbutsev, I.V. Molodtsova, and P. Schuck, *Phys. Rev. C* **97** (2018) 044316.
- [10] P. Ring and P. Schuck, *The Nuclear Many-Body Problem*, Springer, Berlin (1980).
- [11] D.A. Varshalovitch, A.N. Moskalev, and V.K. Khersonski, *Quantum Theory of Angular Momentum*, World Scientific, Singapore (1988).
- [12] E.B. Balbutsev, I.V. Molodtsova, and P. Schuck, *Acta Phys. Pol. B Proc. Suppl.* **12**(3) (2019) 637.
- [13] N. Pietralla *et al.*, *Phys. Rev. C* **52** (1995) R2317.
- [14] J. Enders *et al.*, *Phys. Rev. C* **71** (2005) 014306.
- [15] J. Margraf *et al.*, *Phys. Rev. C* **52** (1995) 2439.
- [16] V. Soloviev, A. Sushkov, and N. Shirikova, *Phys. Part. Nucl.* **31** (2000) 385.